A Solid-State Investigation of the Desorption/Evaporation of Hindered Phenols from Low Density Polyethylene Using FTIR and UV Spectroscopy with Integrating Sphere: The Effect of Molecular Size on the Desorption

KENNETH MÖLLER and THOMAS GEVERT

Department of Materials Technology, Swedish National Testing and Research Institute, PO Box 857, S-501 15 Borås, Sweden

SYNOPSIS

Low density polyethylene (LDPE) has been investigated with respect to the desorption/evaporation of hindered phenol antioxidants added to the polymer matrix. In this study, Fourier transform infrared and ultraviolet (FTIR and UV) spectroscopy without any extraction or refining steps in the analysis were used to measure the desorption constants. The UV spectrophotometer was equipped with an integrating sphere. The desorption constants, α, of five phenols containing the same 3,5-di-tert-butyl-4-hydroxyphenyl structure, but differing by the length of the hydrocarbon tails, were obtained in the temperature range of 40–100°C. The number of methylene groups in the tail varied between 0 and 17. The temperature-dependence of the phenols could be described by an Arrhenius type relationship. Very large differences in desorption rates were found due to differences in size of the antioxidants. © 1996 John Wiley & Sons, Inc.

INTRODUCTION

To protect polymers from different kinds of degradation, various additives, such as antioxidants, must often be added to the system. In most cases, the antioxidants are mobile to some extent. Excessive mobility, however, can lead to a serious physical loss of antioxidants from the polymeric material to the surrounding environment, e.g., indoor environment, food, etc., causing undesired implications. As a consequence, knowledge of the nature of the transport phenomena is very important in many respects. The same phenomenon may also have an impact on recycling of polymeric materials. It will probably be necessary to upgrade many recyclates, due to chemical degradation and physical loss of antioxidants, before they can be utilized in new recycled products. It is also very important to consider physical transport processes in accelerated aging tests and lifetime predictions. Reliable predictions will only be derived from tests in which the different degradation mechanisms of a specific polymeric material are accelerated by the same acceleration factor. For these and other reasons, a large number of investigations concerning transport properties of small molecules in polymers have been undertaken in different areas of science.[1-5]

In a previous paper,[6] we have presented the results from an investigation concerning diffusion of antioxidants in low density polyethylene (LDPE). The antioxidants were hindered phenols, all containing the same 3,5-di-tert-butyl-phenyl structure:

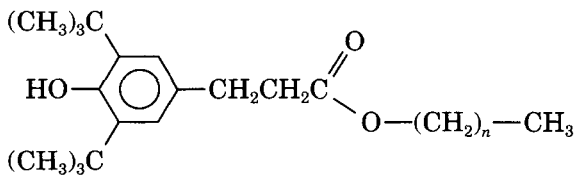

where n, the number of methylene groups, is 0, 2, 5, 11, and 17.

The same five hindered phenols have been used in this investigation, which is focused on the de-

Journal of Applied Polymer Science, Vol. 61, 1149–1162 (1996)
 CCC 0021-8995/96/071149-14

sorption/evaporation of the antioxidants from the surface of polymer films.

The antioxidant with 17 methylene groups is available commercially under the trade name Irganox 1076 and is manufactured by Ciba-Geigy AG, Switzerland. The antioxidants with $n = 0$, 2, 5, and 11 have all been synthesized in our laboratory.

In this study, direct spectroscopic methods were used to measure the desorption constants, i.e., FTIR and UV spectroscopy on solid-state films to avoid any extraction or refining steps in the analysis. The temperature range used in the investigation was 40–100°C.

We have also made an attempt to elucidate the theoretical treatment of the desorption phenomenon and to make a comparison with the findings from the diffusion investigation executed earlier.[6] Thus, a comparison between the importance of diffusion and desorption to the overall loss of antioxidants is presented.

THEORY

The experimental results obtained have been evaluated according to Crank.[7]

$$\frac{M_t}{M_\infty} = 1 - \sum_{n=1}^{\infty} \frac{2L^2 \exp(-\beta_n^2 Dt/l^2)}{\beta_n^2(\beta_n^2 + L^2 + L)} \tag{1}$$

where M_t is the amount of desorbing species which has left the film after time t; M_∞, the corresponding quantity after infinite time, which in this case is also equal to the initial amount; and D, the diffusion coefficient. The β_n:s are the positive roots of

$$\beta \tan \beta = L \tag{2}$$

where L is defined as

$$L = l\alpha/D \tag{3}$$

$2l$ is the film thickness; and α, the desorption or evaporation constant. Desorption/evaporation, as well as sorption processes, obey eq. (1).

Equation (1) is the solution to the coupled differential equations

$$\frac{\partial c}{\partial t} = D \frac{\partial^2 c}{\partial x^2} \tag{4}$$

and

$$-D \frac{\partial c}{\partial x} = \alpha(c_0 - c_s) \tag{5}$$

where c_s is the concentration just below the surface of the film, and c_0, the concentration just below the surface required to maintain equilibrium with the surrounding atmosphere, which in this case is flowing nitrogen. The variable c_0 can therefore be regarded as equal to zero.

Equation (4), which is Fick's second law of diffusion, describes the diffusion within the film, while eq. (5) describes the evaporation/desorption of antioxidants from the surface of the film to the surroundings. It should perhaps be pointed out that this problem from a mathematical point of view is analogous to heat transport within a solid, with the same geometry, coupled with radiative heat loss at the surface. Carslaw and Jaeger[8] have given the solution to this problem.

Equation (1) is used in the literature[9,10] in the interpretation of desorption experiments and is almost always approximated by the first term. The justification is based on numerical evaluations; see, for example, Calvert and Billingham.[9] However, a theoretical examination, as presented below, clearly demonstrates under which conditions the approximation is true.

Equation (1) can be written as

$$1 - \frac{M_t}{M_\infty} = \sum_{n=1}^{\infty} A_n B_n(t) \tag{6}$$

where A_n and B_n are defined by eq. (1) as

$$A_n = \frac{2L^2}{\beta_n^2(\beta_n^2 + L^2 + L)} \tag{7}$$

$$B_n(t) = \exp(-\beta_n^2 Dt/l^2) \tag{8}$$

For reasons which will be obvious later, the function

$$\beta^2 = f(L) \tag{9}$$

is of interest to obtain (numerically) and examine more closely. One can, for example, notice that the exponential factor in eq. (1), $B_n(t)$, contains $\beta_n^2 D/l^2$, i.e., both β_n^2 and D/l^2. L is, according to eq. (3), proportional to l/D.

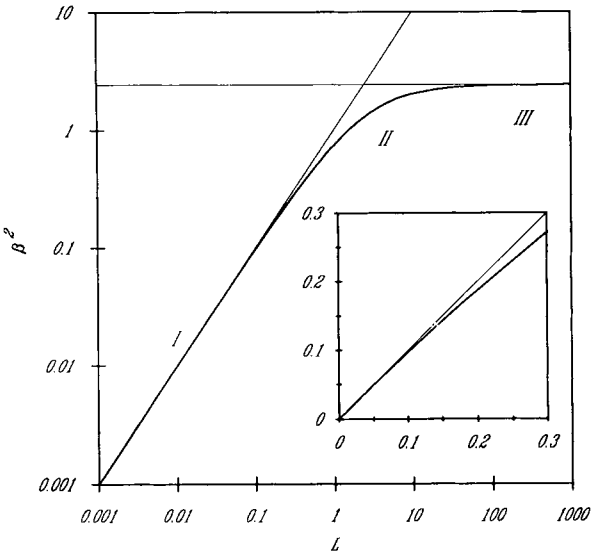

Figure 1 Log-log plot of eq. (9) showing the three different regions. The straight lines represent eq. (10) and eq. (11), respectively. Region I is shown in linear scales in the insert.

Equation (9) is found by solving eq. (2) numerically, i.e., obtaining the inverse ($\beta = f(L)$) of eq. (2), and then squaring the β values. In Figure 1, $\beta^2 = f(L)$ is shown for n equal to 1. As is seen in the figure, three different regions can be identified. At small values of L ($L < 0.1$), (region I), the function asymptotically approaches the straight line

$$\beta^2 = L \tag{10}$$

while at large values ($L > 50$), (region III), the function asymptotically approaches the straight line

$$\beta^2 = \frac{\pi^2}{4} = 2.4674 \tag{11}$$

In Region II ($0.1 < L < 50$), the function cannot, of course, be approximated by a straight line as is seen in Figure 1.

Region I

As stated above, eq. (10) is obtained by a numerical solution of eq. (2). It can, however, easily be obtained from a more "mathematical" point of view. $\tan \beta$ can be expanded as

$$\tan \beta = \beta + \frac{\beta^3}{3} + \frac{2\beta^5}{15} + \frac{17\beta^7}{315} + \cdots \tag{12}$$

For small values of β, one gets

$$\tan \beta = \beta \tag{13}$$

Equation (13) inserted into eq. (2) gives eq. (10).

By combining eqs. (3), (8), and (10), one gets for $n = 1$

$$B_1(t) = \exp(-\beta_1^2 Dt/l^2) = \exp(-\alpha t/l) \tag{14}$$

At small values of L, the preexponential factor of the first term, A_1, in eq. (1) or (7) becomes

$$A_1 = \frac{2L^2}{\beta_1^2(\beta_1^2 + L^2 + L)} = \frac{2}{2 + L} \cong 1 \tag{15}$$

after insertion of eq. (10) for $L \ll 1$.

The preexponential factor in the first term equals, for example, 0.95 for $L = 0.1$ and 0.99 for $L = 0.03$. Since the sum in eq. (1) must, of course, be equal to unity at time zero, the preexponentials in higher terms must be very small for small values of L. In Figure 2, the first four preexponential factors ($A_1 - A_4$) are shown as a function of L. As the value of n increases in the sum [eq. (1)], the values of the corresponding exponential factors [$B_n(t) = \exp(-\beta_n^2 Dt/l^2)$] as a function of time rapidly decreases, since $\beta_{n+1} > \beta_n$. Consequently, only the first term in eq. (1) is needed for small values of L.

For small values of L, eq. (1) can be written

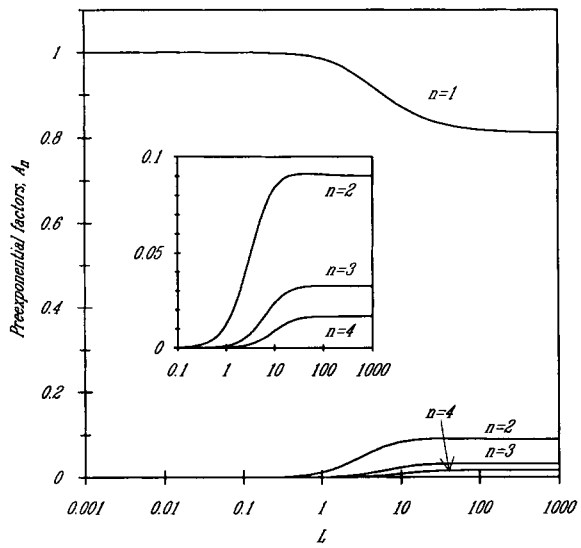

Figure 2 The first four preexponential factors A_n as a function of L.

$$1 - \frac{M_t}{M_\infty} = A_1 \exp\left(-\frac{\alpha}{l} t\right) \qquad (16)$$

or

$$\ln\left(1 - \frac{M_t}{M_\infty}\right) = \ln A_1 - \frac{\alpha}{l} t \cong -\frac{\alpha}{l} t \qquad (17)$$

since A_1 is close to unity. If $\ln\left(1 - \frac{M_t}{M_\infty}\right)$ is plotted as a function of exposure time, t, the slope of the straight line [eq. (17)] is equal to $\frac{\alpha}{l}$.

At sufficient small values of L, the loss rate is completely determined, according to eq. (14), by the desorption from the surface of the film and not by the diffusion inside the film. As a consequence, only α can be determined in this region.

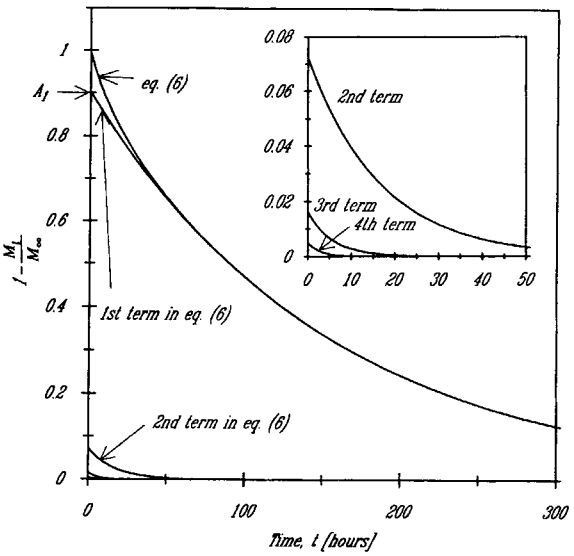

Figure 3 A plot of eq. (6) for L equal to 6 (D = 1.0 $\times 10^{-14}$ m^2/s and l = 0.1 mm).

Region II

In region II ($0.1 < L < 50$), the function is markedly curved (see Fig. 1). In this region, the value of the first preexponential factor, A_1, decreases from 1 to $8/\pi^2 = 0.81$. At the same time, the values of higher preexponentials increase (see Fig. 2). At the least, the second term can contribute significantly to the sum in this region. However, since the exponentials, $B_n(t)$, from higher terms decrease much more rapidly as a function of time compared to the first term ($\beta_{n+1} > \beta_n$), the contribution from higher terms to the sum decreases rapidly as a function of time. In Figure 3, eq. (6) is shown for an L value equal to 6, i.e., a value in the middle of Region II. In the same figure, the contribution from the first four terms is also shown. As is seen, the contribution from higher terms can be neglected when the quantity of desorbing species remaining in the film has decreased to about 75% of the initial amount. For lower values or corresponding longer periods of exposure, the sum and the first term coincide, so the contribution from higher terms can be neglected. In Figure 4, $\ln\left(1 - \frac{M_t}{M_\infty}\right)$ is plotted versus exposure time. The first term as well as the sum [eq. (6)] is shown in the figure. The slope of the straight line part of the sum is equal to the slope of the logarithm of the first term, which is equal to $-\beta_1^2 D/l^2$. The intercept of the $\ln\left(1 - \frac{M_t}{M_\infty}\right)$-axis of the straight line is equal to $\ln A_1$. If the value of A_1 is known eqs. (2) and (7) can be used to calculate the values of β_1 and L. The slope of the straight line and the value of β_1 give, of course, the value of D if l, the thickness of the film, is known. Knowing the values of D and L, α can be calculated according to eq. (3). Thus, in region II, α and D can be simultaneously determined. However, a serious problem arises. A_1 can only have a value between 1 and 0.81. At the same time, L varies between zero and infinity, so that small changes in A_1 correspond to large changes in L. A_1 must therefore be determined with an extremely high degree of accuracy, which is very difficult to achieve. Only the product $\beta_1 D$ can be determined with high accuracy. However, if one of the parameters D or α is known, the other can be calculated.

Region III

The value of β for the first root of eq. (2) varies between 0 and $\pi/2$. As β_1 goes to $\pi/2$, $\tan \beta_1$ goes to infinity. This means that for large values of L, β_1 is close to $\pi/2$ and, consequently, β_1^2 is close to $\pi^2/4 = 2.4674$, i.e., eq. (11).

By combining eqs. (8) and (11), one gets

$$B_1(t) = \exp(-\beta_1^2 Dt/l^2)$$
$$= \exp(-\pi^2 Dt/4l^2) \qquad (18)$$

This means that at sufficiently large values of L, the loss rate is determined, according to eq. (18), by the diffusion inside the film and not by the evaporation from the surface.

The same arguments used concerning region II can be used concerning Region III. One difference,

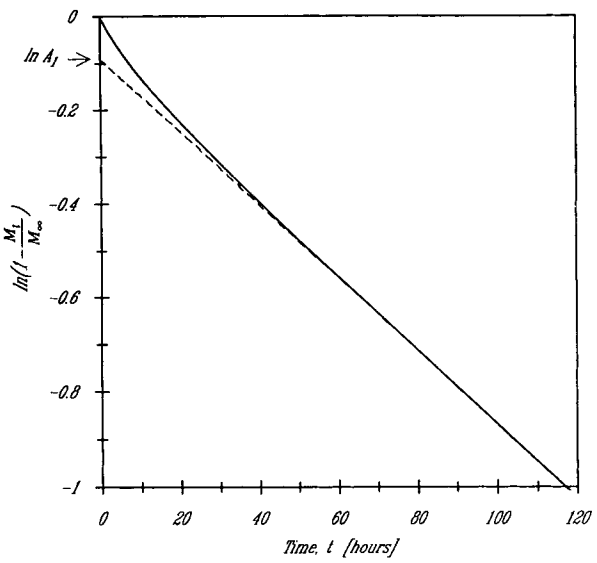

Figure 4 $\ln\left(1 - \frac{M_t}{M_\infty}\right)$ plotted versus exposure time t. The logarithm of the first term is also included (straight, broken line). The intercept of the $\ln\left(1 - \frac{M_t}{M_\infty}\right)$-axis of the straight line is equal to $\ln A_1$.

however, is that the slope is now equal to eq. (18). Another difference is that the intercept is equal to or very close to A_1 ($8/\pi^2 = 0.81$). In region III, only D can be determined.

As discussed, three different regions can be identified. In the first region, the loss of additive is controlled by desorption from the surface of the sample. In an intermediate region, both desorption and diffusion are of importance. Finally, in the third region, the loss is controlled by diffusion inside the sample. Calvert and Billingham[9] have also identified the different regions discussed above. However, their approach was based on the approximation that degradation and failure of polymeric materials proceeds rapidly when the average concentration of additive falls below 10% of the initial value.

EXPERIMENTAL

Materials

The low density polyethylene used was the same as used in a previous study.[6] It was produced by Borealis Polyeten AB, Sweden (grade NCPE 6600). The weight average molecular weight M_w was 1.03×10^5 g/mol, and the number average M_n was 2.22×10^4 g/mol. The density, ρ, was 922 kg/m^3. This value corresponds to the volume crystallinity $\alpha_v = (\rho - \rho_a)/(\rho_c - \rho_a)$ equal to 0.47 or to the mass crystallinity $\alpha_m = \rho_c(\rho - \rho_a)/\rho(\rho_c - \rho_a) = \alpha_v\rho_c/\rho$ equal to 0.51. The values[11] of ρ_a and ρ_c are equal to 853 and 1000 kg/m^3, respectively. Borealis has reported the polyethylene to be free from additives. However, the infrared spectrum of this material does contain a band at 1720 cm^{-1}, which most probably originates from ketone used as a chain transferring agent in the polymerization process.

The largest phenol used, Irganox 1076, was purchased from Ciba-Geigy AG, Switzerland. The other four were synthesized in-house. The syntheses of the alkyl esters are briefly described elsewhere.[6]

In general, samples have to be conditioned before exposure in aging experiments. For samples only stored in a refrigerator prior to exposure in test cells, we could initially observe a deviation from the ideal exponential decay loss process. This deviation was, however, quite short compared to the total duration of exposure. In order to minimize this effect, the films used throughout this investigation were placed in a stack of similar films and heated in an oven for at least five hours at the exposure temperature before they were placed in a test cell. For these conditioned films, we did not observe any deviation from the theoretical exponential decay loss process.

Test Equipment

For the larger antioxidants, the evaporation rate is very low. This means that the duration of a measurement is quite long, on the order of 10^3 h. When exposed to air for such a long period of time at high temperatures, polyethylene films can suffer degradation even if they contain antioxidants. Since we wanted to investigate transport properties only, the films had to be protected from oxidative degradation. To achieve this, small test cells were constructed through which pure nitrogen was passed. The dimensions of the cells were $100 \times 100 \times 10$ mm. The cells were made quite small to minimize the nitrogen consumption. The linear flow rate of the nitrogen gas was 10 mm/s. The purity of the nitrogen used was better than 99.9999%. The test cells were placed in ovens. The temperatures chosen were 40, 50, 70, 80, 90, and 100°C. The true oven temperatures were measured with carefully calibrated Pt100 sensors. The temperatures were also continuously recorded. The deviation in temperature from the set values given above was ±0.3°C. Before the nitrogen gas entered the test cells, the gas was heated in a heat exchanger placed in the same oven as the test cell. The temperatures of the inlet gas to the cells were

also measured and compared with the oven temperatures. No significant deviations were found.

Measuring Procedures

The additive content was determined by FTIR and UV spectroscopy directly on the films; i.e., no extraction was used. The advantage is that the films can be put into the testing cells again, and the test can continue.

Films containing antioxidants were prepared from additive-free PE-pellets by a moulding procedure described elsewhere.[6] By moulding films instead of using film-blowing techniques, we believe that orientation effects in the polymer matrix may be avoided. It has been shown[12] that orientation of the polymer chains can affect the diffusivity of additives.

The concentration of the antioxidant in the film was determined from absorbance spectra obtained by an FTIR spectrophotometer (Mattson Cygnus 100) and by an UV-VIS-NIR spectrophotometer (Perkin-Elmer Lambda 9) equipped with an integrating sphere.

The ester band at 1740 cm^{-1} in the FTIR spectra was used as a measure of the antioxidant concentration. We also used a spectral subtraction technique, which is described in detail elsewhere.[6]

A serious problem did arise, however, in using FTIR spectroscopy. Although the polyethylene films were exposed to pure nitrogen, tracer amounts of oxygen caused a slight oxidation of the samples at high temperatures and long exposure times (>1500 h). The oxidation products gave rise to absorption bands in the IR region at almost the same wave number as the antioxidants, thus causing a severe interference. To overcome this problem, we also used UV spectroscopy with an integrating sphere attachment.

In UV spectroscopy on solid materials, especially semicrystalline materials like polyethylene, problems caused by light scattering and reflection occur, which have limited its use. Luongo[13] has, however, demonstrated the feasibility of UV spectroscopy directly on polymer films. He was able to determine additive levels ranging from 0.002 to 1.00% in polyethylene for a number of additives.

If problems with scattering and reflection can be avoided, UV spectroscopy has great advantages in quantitative analysis of additives in polyolefines due to high sensitivity and lack of interference from the polymer matrix. Albarino[14] has successfully demonstrated that the problems arising from scattering can be effectively reduced by melting the sample, thus eliminating the scattering crystallites. He was investigating an antioxidant, Irganox 1010, in polyethylene.

An alternative method in eliminating the negative effects of light scattering is to use an integrating sphere attachment, which collects all transmitted light. Reflected light can also be collected (see below).

In absorption spectroscopy transmittance τ is defined as

$$\tau(\lambda) = \frac{\phi(\lambda)}{\phi_0(\lambda)} \tag{19}$$

where $\phi_0(\lambda)$ = intensity of incident radiant flux
$\phi(\lambda)$ = intensity of transmitted radiant flux
λ = wavelength

In ordinary IR and UV-VIS spectroscopy, $\phi(\lambda)$ is the transmitted radiant flux detected in the direction of incidence. In UV-VIS spectroscopy, light scattering during transmission through semicrystalline polymeric materials, such as polyethylene, is very pronounced as pointed out above.

We can redefine the quantity $\phi(\lambda)$ as

$$\phi(\lambda) = \phi_{TI}(\lambda) + \phi_{TS}(\lambda) + \phi_R(\lambda) \tag{20}$$

where $\phi_{TI}(\lambda)$ = intensity of transmitted radiant flux in the direction of incidence (regular transmittance)
$\phi_{TS}(\lambda)$ = intensity of transmitted radiant flux which is scattered when passing the sample (diffuse transmittance)
$\phi_R(\lambda)$ = intensity of reflected (specular and diffuse) radiant flux

We now define $\tau_I(\lambda)$, $\tau_S(\lambda)$, and $\rho(\lambda)$ as

$$\tau_I(\lambda) = \frac{\phi_{TI}(\lambda)}{\phi_0(\lambda)} \tag{21}$$

$$\tau_S(\lambda) = \frac{\phi_{TS}(\lambda)}{\phi_0(\lambda)} \tag{22}$$

$$\rho(\lambda) = \frac{\phi_R(\lambda)}{\phi_0(\lambda)} \tag{23}$$

$\tau_I(\lambda)$, $\tau_S(\lambda)$, and $\rho(\lambda)$ are transmittance in incident direction (regular transmittance), scattered (diffuse) transmittance, and (total) reflectance, respectively.

Often, in spectroscopy, only $\tau_I(\lambda)$ is obtained. The contribution from $\tau_S(\lambda)$ and $\rho(\lambda)$ is neglected. The neglection of $\tau_S(\lambda)$ and $\rho(\lambda)$ results in a background,

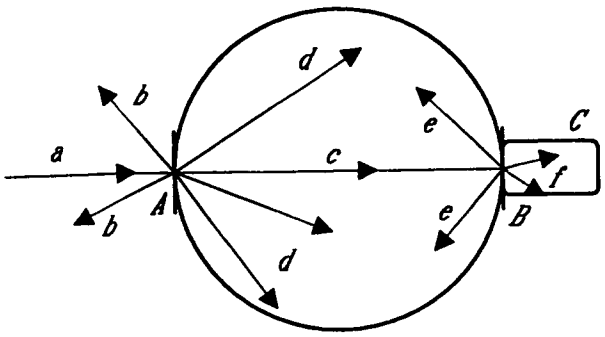

Figure 5 Schematic drawing of an integrating sphere. The sample is placed at the entrance port *A*, when obtaining a transmission spectrum. At the same time, a reflector is placed at the exit port *B*. When a reflectance spectrum is obtained, the sample is placed at the exit port together with the radiant trap *C*. *a* denotes incident radiation; *b* and *e* denote reflected radiation; *c* is regular transmittance; *d* and *f* are scattered transmission radiation.

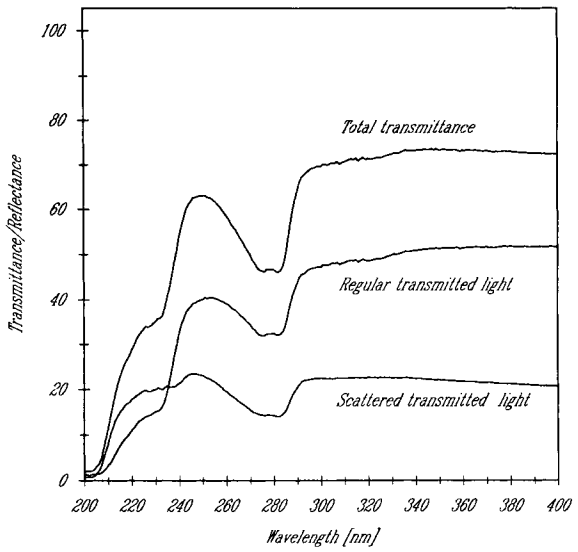

Figure 6 Transmittance UV spectra obtained with an integrating sphere for Irganox 1076 (0.1 wt %). Total transmittance, as well as scattered and regular transmittance, are shown.

which differs from the 100% transmittance level, but also in a decrease in obtained absorption bands intensities. These effects are of minor importance when working with, for example, nonturbid solutions.

In Figure 5, the schematic drawing shows the basic principles of an integrating sphere. In order to obtain a transmittance spectrum, the sample (LDPE film) is placed at the entrance port of the sphere. In principle, all radiation passing the sample is collected by the sphere.

Figure 6 shows the effect of light scattering. As can be seen, the major contribution to the total transmittance originates from the regular transmittance. However, the contribution from regular transmittance decreases as a function of film thickness. Normally, the concentration of antioxidants in polyolefines is quite low, about 0.1 wt %. To increase the signal, i.e., the band intensity in an UV spectrum, the path length or film thickness can be increased, for example, by folding the film.

By using an integrating sphere, the reflected part of the incident radiation can also be obtained. In fact, integrating spheres are usually used to obtain reflectance spectra.[15,16] The sample is placed at the exit port, also called reflectance port. Behind the sample, a radiation trap is placed, see (Fig. 5). A radiation trap is often a cavity having black internal surfaces which absorb all radiation entering the trap. In that way, only radiation reflected by the sample is collected by the sphere, i.e., $\rho(\lambda)$ [eq. (23)] is obtained.

Spectra from samples at the entrance and exit ports can now be added. In the resulting spectrum, essentially all effects of scattering and reflection are removed (see Fig. 7). This spectrum is then transformed to an absorbance spectrum. In Figure 8, an example of such a spectrum is shown. As can be seen, the baseline is very close to zero, and the spectrum has a very good signal to noise ratio. By obtaining the second derivative of the absorbance spectrum, the resolution can be increased (see Fig.

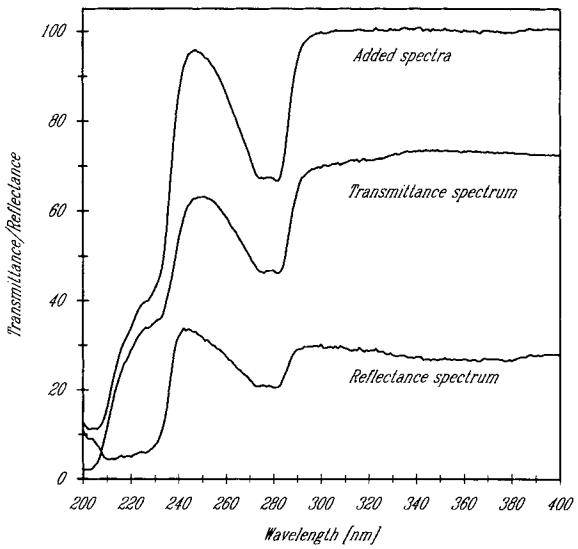

Figure 7 Transmittance and reflectance spectra for Irganox 1076 (0.1 wt %). The added spectrum is also shown.

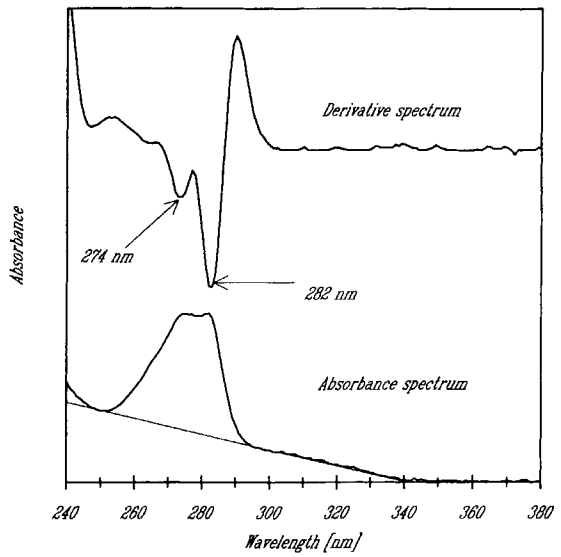

Figure 8 Absorbance spectrum for Irganox 1076 (0.1 wt %). The second derivative spectrum is also shown.

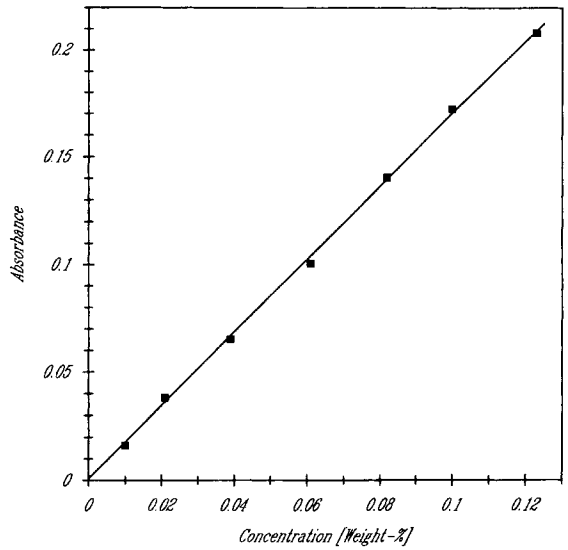

Figure 9 Absorbance versus known film concentration, i.e., a calibration curve, for Irganox 1076 with a film thickness of 200 μm.

8). Two distinct bands can now be identified (274 and 282 nm), as is seen in Figure 8. These bands originate from the substituted phenolic group[17] in the antioxidant molecule. The peak height at 282 nm was used as a measure of the antioxidant content in the films.

Figure 9 shows a plot of absorbance versus known film concentration, i.e., a calibration curve, for Irganox 1076 with a film thickness of 200 μm. As can be seen, the plot can be represented by a straight line with an intercept very close to the origin, demonstrating that the Beer–Lambert law is obeyed. Similar calibration curves were obtained for all the five antioxidants, and the various film thicknesses used.

The initial mole concentration in the films was the same for all five antioxidants. The weight concentration for the octadecylester (Irganox 1076) was 0.1%, which corresponds to the concentration commonly used in practical applications.

RESULTS AND DISCUSSION

Figure 10 exemplifies the loss of antioxidants as a function of time. The experimental conditions (film thickness) were chosen in such a way that eq. (17) (region I) could be used in the evaluation of the desorption constant, α. The solid line represents the best fit according to eq. (17).

As can be seen in Figure 10, there are no significant differences in the results obtained by IR and UV spectroscopy for exposure times of about 1500 h or less at 100°C for the loss of the dodecylester ($n = 11$). However, after 1500 h, there is a deviation. In fact, IR spectroscopy indicates an increase in the antioxidant content (see Fig. 10). A reasonable explanation to the increase in intensity of the 1740 cm^{-1} band is oxidation of the polymer caused by tracer amounts of oxygen. The oxidation does not, however, cause any interference with the UV mea-

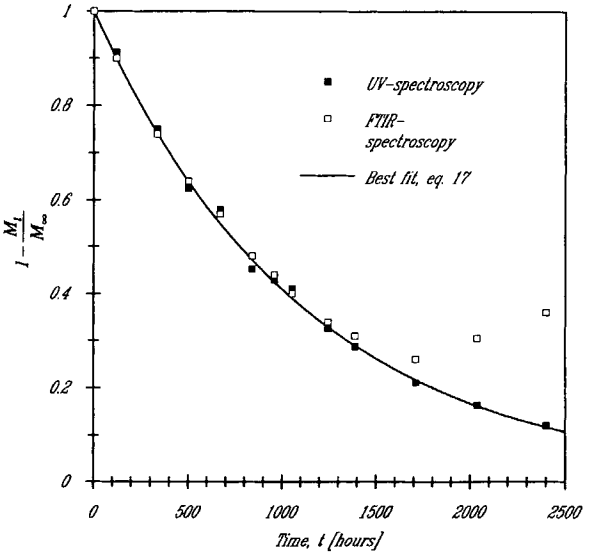

Figure 10 $1 - \frac{M_t}{M_\infty}$ plotted versus exposure time t for the dodecylester ($n = 11$). The symbols are explained in the figure.

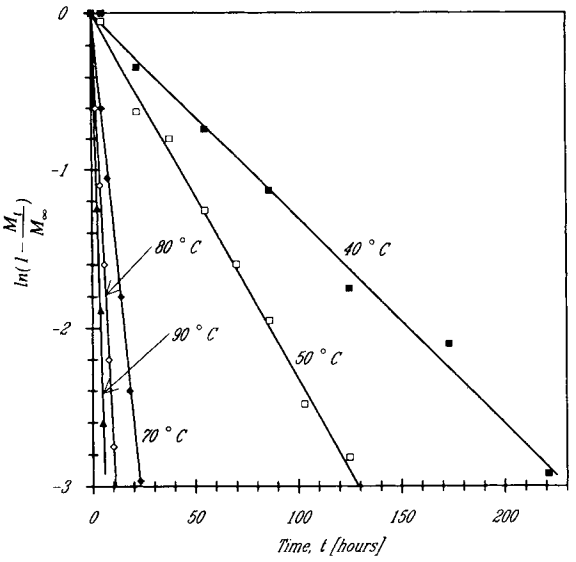

Figure 11 $\ln\left(1-\frac{M_t}{M_\infty}\right)$ plotted versus exposure time t for the methylester (n = 0). Exposure temperatures are given in the figure. The straight lines represent the best least linear square fits according to eq. (17).

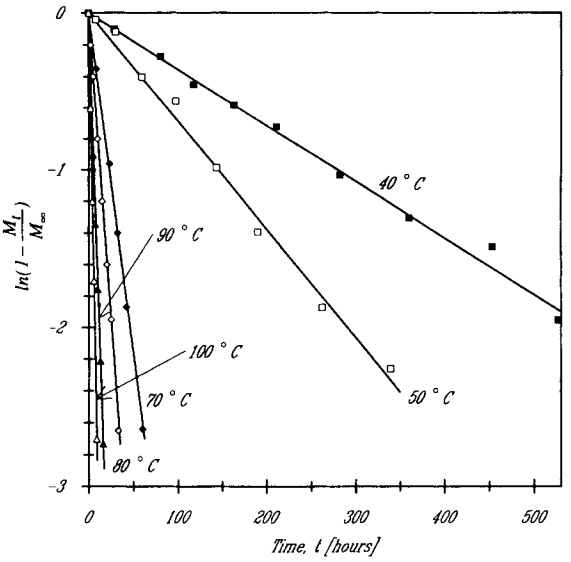

Figure 12 $\ln\left(1-\frac{M_t}{M_\infty}\right)$ plotted versus exposure time t for the propylester (n = 2). Exposure temperatures are given in the figure. The straight lines represent the best least linear square fits according to eq. (17).

surements since the absorption of UV radiation is caused by the aromatic part of the antioxidant.

In Figures 11–14, all results are plotted according to eq. (17). As can be seen, the data points can be fitted nicely to straight lines.

Due to experimental demands, the thickness of the films had to be varied, depending on the size of the antioxidant and the temperature of the experiment. At high temperatures and with the smallest antioxidants, the loss rates were very high. To keep overall exposure times long enough that the time required for thermal equilibration was not significant, the films had to be quite thick, about 200 μm. The shortest exposure time was about 10 h. On the other hand, for larger antioxidants and lower temperatures, the loss rate was so low that we had to use thinner films in order to achieve reasonable exposure times. The maximum exposure times were about 2600 h. The thinnest films used were 50 μm thick.

Our goal was to follow the desorption loss process down to very low concentrations so that we could determine not only the loss rate but also the shape of the desorption loss rate curve. This was, however, not possible for the largest antioxidants. As a matter of fact, only the initial part of the loss curve at 100°C could be determined for Irganox 1076.

In Table II, the determined values of α are given. By using eq. (3), the L values can be obtained using the values of the diffusion coefficient, D, given in Table I. The values of L are also given in Table II. As can be seen from Table II, the L values are small, indicating a more or less pure desorption regime; i.e., the loss rate is dominated by desorption from the surfaces and not by diffusion within the films (i.e., region I).

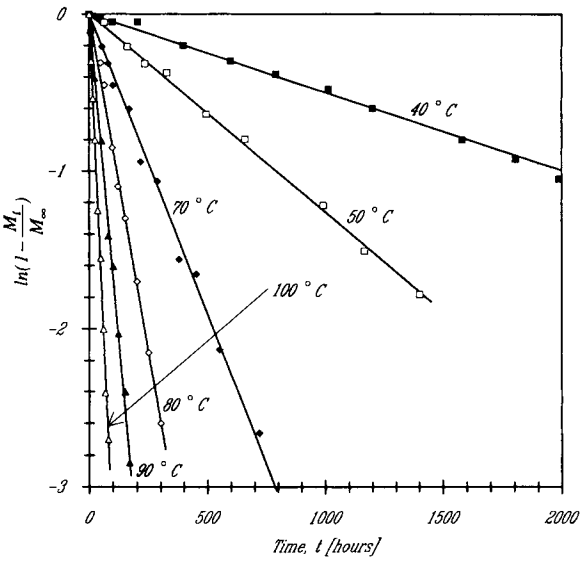

Figure 13 $\ln\left(1-\frac{M_t}{M_\infty}\right)$ plotted versus exposure time t for the hexylester (n = 5). Exposure temperatures are given in the figure. The straight lines represent the best least linear square fits according to eq. (17).

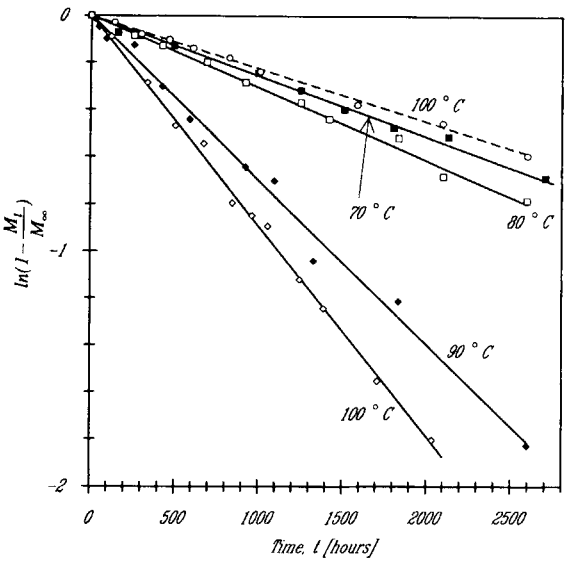

Figure 14 $\ln\left(1-\frac{M_t}{M_\infty}\right)$ plotted versus exposure time t for the dodecylester and the octadecylester (n = 11 and 17, respectively). Exposure temperatures are given in the figure. The solid straight lines represent the best least linear square fits according to eq. (17) for the dodecylester. The broken line represents the best fit for the octadecylester, which was investigated at 100°C only.

In Figure 15, the obtained values of the logarithm of α are plotted as a function of reciprocal absolute temperatures, $1/T$, for the five antioxidants. As can be seen from Figure 15, all plots can be represented by straight lines (in the case of Irganox 1076, it is of course self evident since there is only one point). The results indicate that the temperature dependence of the desorption can be represented by an Arrhenius type relation

$$\alpha = \alpha_0 \exp(-E_\alpha/RT) \qquad (24)$$

where α_0 is the preexponential factor; E_0, the activation energy; R, the universal gas constant; and T, the temperature.

The activation energies, E_α, and preexponential factors, α_0, for all antioxidants, except for the largest one (Irganox 1076), are calculated from best-fitted straight lines. The obtained values of α_0 and E_α are given in Table III.

In Figure 16, the activation energy, E_α, is plotted versus the number of methylene groups, n, in the tail of the four lightest antioxidants. As can be seen in Figure 16, the correlation can be well approximated by a straight line. The activation energy for the largest antioxidant can now be obtained by extrapolation. The extrapolated value is included in Table III. As is also seen from Table III, the values of the preexponential factors are almost the same for the five antioxidants. This is in contrast to the findings for the diffusion coefficients reported in our previous work,[6] where we found an exponential correlation between the preexponential factors and the size of the antioxidants. The mean value of the four obtained preexponential factors are given as the preexponential for the largest antioxidant in Table III. It is often dangerous to extrapolate values as we have done for the desorption parameters of Irganox 1076. We are, however, in a position in which we can check the extrapolation since we have obtained a measured value of α for Irganox 1076 at 100°C. The calculated α-value at 100°C is 1.35×10^{-12} m/s, which should be compared with the corresponding value given in Table II (1.57×10^{-12} m/s). The deviation is quite small, which supports the extrapolation done above.

Table I Diffusion Coefficients D of Hindered Phenols[a] in LDPE

Diffusant[a]	No. Methylene Groups (n)	Molar Mass (M) (g/mol)	$D \times 10^{14}$ m²/s (Temperature, °C) 40[c]	50[c]	70[d]	80[d]	90[d]	100[d]
Methylester	0	292	21.7	51.2	367	708	1360	2320
Propylester	2	320	19.1	44.8	326	657	1220	2260
Hexylester	5	362	16.1	41.9	295	685	1030	1780
Dodecylester	11	446	11.6	34.3	241	532	868	1460
Octadecylester[b]	17	530	8.57	19.0	170	371	690	1180

[a] Alkyl esters of 3,5-di-tert-butyl-4-hydroxyl-phenyl propionic acid.
[b] Irganox 1076.
[c] From Möller and Gevert.[6]
[d] The values of D are obtained according to the method used in Möller and Gevert[6].

Table II Desorption Constants α of Hindered Phenols[a] from LDPE Films and Corresponding L Values (200 μm Thick Films)

Desorbing[a] Species	No. Methylene Groups (n)	Molar Mass (M) (g/mol)	$\alpha \times 10^{11}$ m/s and $(L = \frac{l\alpha}{D})$ (Temperature, °C)						
			40	50	70	80	90	100	
Methylester	0	292	36.2 (0.17)	64.5 (0.13)	361 (0.10)	756 (0.11)	1410 (0.10)	—	
Propylester	2	320	9.94 (0.05)	19.1 (0.04)	121 (0.04)	217 (0.03)	472 (0.04)	828 (0.04)	
Hexylester	5	362	0.690[c] (0.002)	1.75[c] (0.002)	10.6 (0.004)	24.0 (0.003)	46.5 (0.005)	94.5 (0.005)	
Dodecylester	11	446	—	—	0.179[d] (2×10^{-5})	0.427[c] (2×10^{-5})	0.970[c] (6×10^{-5})	2.48 (2×10^{-4})	
Octadecylester[b]	17	530	—	—	—	—	—	0.157[d] (3×10^{-8})	

[a] Alkyl esters of 3, 5-di-tert-butyl-4-hydroxy-phenyl propionic acid.
[b] Irganox 1076.
[c] The film thickness is 100 μm (l = 50 μm).
[d] The film thickness is 50 μm (l = 25 μm).

The so-called compensation effect that we found in the case of diffusion is not present in desorption/evaporation. This means that the desorption constants vary much more as a function of molecular size than the corresponding diffusion coefficients.

We think it is of great importance to compare diffusion and desorption processes. The results of this investigation and the one reported in our previous work[6] show that diffusion within the polymer is a relatively rapid process and not very dependent on molecular size. The ratio in diffusivity between the smallest and largest antioxidant is about 4 at 40°C and only about 2 at 80°C. The desorption, on the other hand, is very dependent on molecular size, and it is very slow for the largest molecules. The ratio in desorption constant between the smallest and largest antioxidant is about 3000 at 80°C and is estimated to be on the order of 10^5 at 40°C.

In Figure 17, the amount of antioxidants still left, in a 0.2 mm thick LDPE film surrounded by pure LDPE at a temperature of 100°C, is plotted as a function of exposure time. The curves represent calculated values according to eq. (1) in our previous work.[6]

$$c = \frac{1}{2} c_0 \left(\text{erf} \frac{h - x}{2(Dt)^{1/2}} + \text{erf} \frac{h + x}{2(Dt)^{1/2}} \right) \quad (25)$$

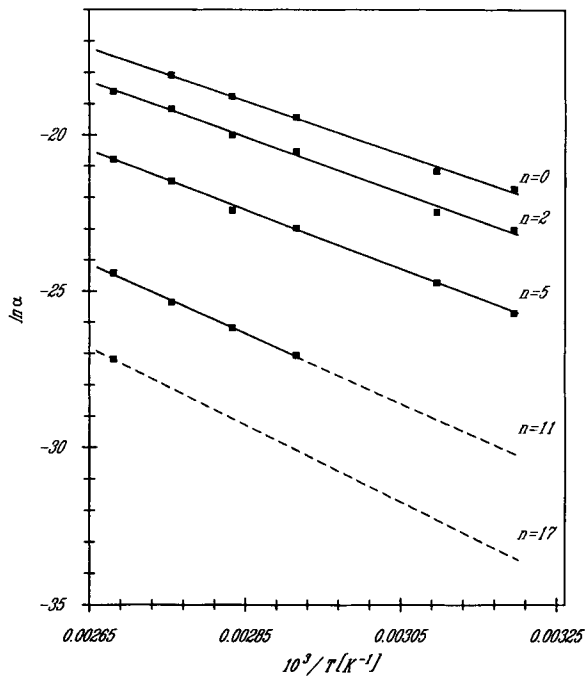

Figure 15 Plots of ln α vs. $1/T$ for the five antioxidants. The broken lines represent extrapolated or estimated values.

Table III Activation Energies E_α and Preexponential Factors α_0 for Desorption of Hindered Phenols[a] in LDPE

Desorbing[a] Species	No. Methylene Groups (n)	Molar Mass (M) (g/mol)	Activation Energy, (E_α) (kJ/mol)	Preexponential Factor (α_0) (m/s)
Methylester	0	292	70.9	216
Propylester	2	320	74.2	218
Hexylester	5	362	78.9	106
Dodecylester	11	446	92.0	136
Octadecylester-Irganox 1076	17	530	103[b]	169[c]

[a] Alkyl esters of 3,5-di-tert-butyl-4-hydroxy-phenyl propionic acid.
[b] Estimated value from Figure 16.
[c] Estimated value. It is the mean value of the four other values given in the table.

where c is the concentration, c_0 is the initial concentration, D is the diffusion coefficient, $2h$ is the total thickness of the doped films, x is the distance, t is the time, and erf is the error function.

The values of the diffusion coefficients are taken from Table I. The corresponding results are shown in Figure 18 for the case in which the film is surrounded by flowing nitrogen (10 mm/s). The curves represent calculated values according to eq. (16). The values of the desorption constants are taken from Table II or calculated according to eq. (24). The values of the parameters in eq. (24) are taken from Table III.

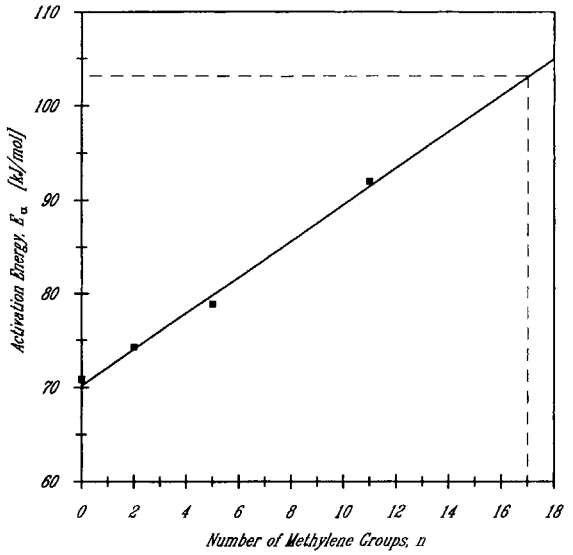

Figure 16 The activation energy E_α as a function of the number of methylene groups n in the hydrocarbon tail of the antioxidants. The straight line represents the best least square fit. The extrapolated value for n equal to 17 (Irganox 1076) is 103.2 kJ/mol.

Two features are obvious when comparing Figures 17 and 18. First, in the case of diffusion, the difference in behavior is quite small between the antioxidants (see Fig. 17). This is in contrast to the behavior in Figure 18, where the differences are very pronounced. In order to plot all five curves in the same figure, we have to use a logarithmic scale on the x-axis. Second, the time needed to reach low antioxidant concentrations is very short only when controlled by diffusion. When desorption is limiting, the time needed to reach a comparatively low concentration is much longer, except for the smallest antioxidant.

Calvert and Billingham[9] have proposed as an approximation that degradation starts when the con-

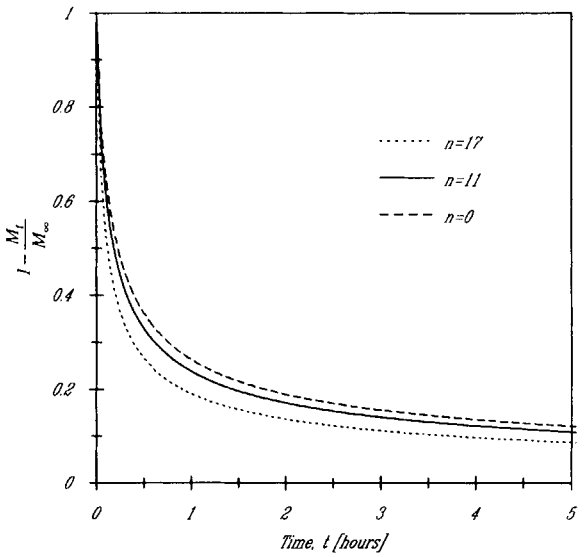

Figure 17 Estimated loss of antioxidants from a 0.2 mm thick LDPE film by diffusion to surrounding pure LDPE at 100°C. Only curves for n equal to 0, 11, and 17 are shown.

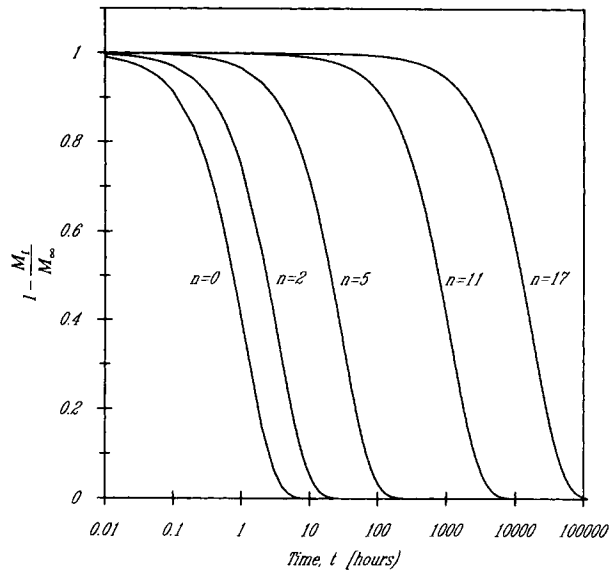

Figure 18 Estimated loss of antioxidants from a 0.2 mm thick LDPE film by desorption (and diffusion) to surrounding flowing nitrogen at 100°C.

centration of antioxidant has dropped below a critical value of about 10% of the initial value. We further assume that, when started, the degradation proceeds very rapidly, so that the life time of a polyethylene film containing antioxidant is completely determined by the physical loss of antioxidant. In reality, this is not true, of course. Antioxidants are consumed by their protective action. If we, in this hypothetical discussion, assume that the service life of a film is only due to physical loss of the antioxidant and apply the 10% limit suggested by Calvert and Billingham, Table III contains all the information needed for estimating service life times for all temperatures and all film thicknesses.

A commonly used accelerated aging qualification test for LDPE film used in buildings as barrier layers is to expose the film to circulating air at 100°C for 4000 h.[18] To be qualified, mechanical properties like elongation at break should not decrease below a critical value. As stated above, degradation of mechanical properties starts and proceeds very rapidly when the antioxidant concentration has reached the critical value.

As is seen in Figure 18, showing the calculated physical loss at 100°C, the concentration of antioxidants with n equal to 0–11 has reached the critical value long before the completion of the qualification test. Films protected by these antioxidants might therefore fail to qualify in such a test.

On the other hand, calculated physical loss at 25°C, which corresponds to natural aging conditions (25°C) is shown in Figure 19. According to this figure, the dodecylester antioxidant (n = 11) concentration has dropped to about 70% of the initial value after about 100 years. The film would thus still be protected if physical loss were the only process consuming antioxidants. The life time, therefore, exceeds 100 years, which must be regarded as very acceptable. There is, consequently, a contradiction between the natural aging (25°C) and the qualification test (100°C, 4000 h).

It should perhaps be noted that dodecylester antioxidant is not a commercial product, so the discussion above is hypothetical. Moreover, the critical antioxidant level above can be discussed, as previous studies have shown that very low concentrations of antioxidant can give protection.[19] The discussion does, however, demonstrate the importance of considering all important factors affecting the life time of a product when performing accelerated aging tests. Application of a specific lower critical value of antioxidant only changes the focus of interest to more easily desorbing antioxidants. It does not change the substance of the argument.

Finally, we have investigated loss of antioxidants to surrounding flowing nitrogen. The gas velocity was 10 mm/s. We do not, however, suggest that the loss rate or α are independent of the gas velocity. On the contrary, it is likely that there is a correlation between loss rate and gas velocity. Elucidation of such a correlation, however, was outside the scope of this investigation. Our main objective was to

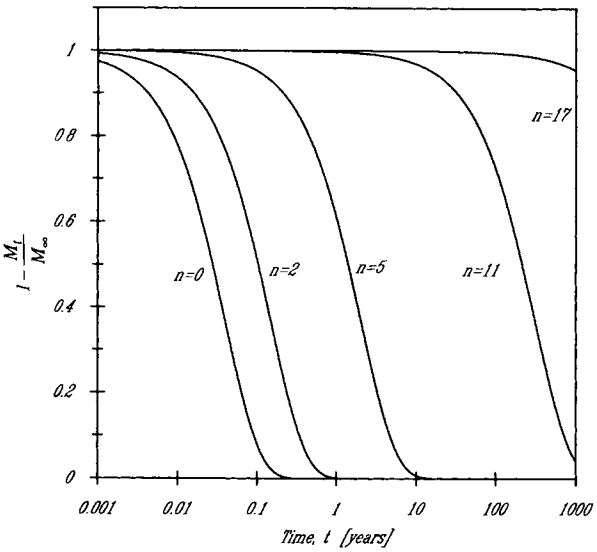

Figure 19 Estimated loss of antioxidants from a 0.2 mm thick LDPE film by desorption (and diffusion) to surrounding flowing nitrogen at 25°C.

demonstrate the influence of molecular size on the loss rate.

CONCLUSIONS

1. It is very difficult, not to say impossible, to determine both α and D in a single experiment.
2. The desorption process is very dependent on molecular size, and it is very slow for the largest molecules. The ratio in desorption constant between the smallest and largest antioxidant in this investigation is about 3000 at 80°C and is estimated to be on the order of 10^5 at 40°C. This result can be compared with the ratio in diffusivity between the smallest and largest antioxidant, which is about 4 at 40°C and only about 2 at 80°C.
3. The results of the investigation show that the temperature dependence of the desorption process can be represented by an Arrhenius type relation.
4. A linear relationship was found between the activation energy, E_α, and the number, n, of methylene ($-CH_2-$) groups in the hydrocarbon tail of the antioxidants.
5. The values of the preexponential factors seem to be more or less the same for the five antioxidants. This finding is contrary to the results obtained for the corresponding preexponential factors for diffusion, where a strong so-called "compensation effect" was found.
6. The lack of "compensation effects" leads to a very pronounced decrease in the values of the desorption constants as a function of the size of the antioxidants. This is contrary to the results obtained for diffusion.
7. At least for thin polyethylene films (<0.1 mm), the loss of antioxidants is controlled by desorption from the surface of the films and not by the diffusion inside the polymeric material.

The authors thank Dr. A. Holmström, Swedish National Testing and Research Institute, for valuable discussions concerning degradation and stabilization of polymers. This work was supported with grants from BFR (the Council for Building Research, Sweden).

REFERENCES

1. J. Comyn, Ed., *Polymer Permeability,* Elsevier, London, 1985.
2. N. E. Schlotter and P. Y. Furland, *Polymer,* **33,** 3323 (1992).
3. J. Crank and G. S. Park, Eds., *Diffusion in Polymers,* Academic Press, London, 1968.
4. G. D. Smith, K. Karlsson, and U. W. Gedde, *Polym. Eng. Sci.,* **32,** 659 (1992).
5. S. Al-Malaika, M. D. R. J. Goonetileka, and G. Scott, *Polym. Deg. Stab.,* **32,** 231 (1992).
6. K. Möller and T. Gevert, *J. Appl. Polym. Sci.,* **51,** 895 (1994).
7. J. Crank, *The Mathematics of Diffusion,* 2nd ed., Clarendon Press, Oxford, 1975.
8. H. S. Carslaw and J. C. Jaeger, *Conduction of Heat in Solids,* 2nd ed., Clarendon Press, Oxford, 1959.
9. P. D. Calvert and N. C. Billingham, *J. Appl. Polym. Sci.,* **24,** 357 (1979).
10. J. Malík, A. Hrivík, and D. Alexyová, *Poly. Deg. Stab.,* **35,** 125 (1992).
11. B. Wunderlich, in *Macromolecular Physics,* Vol. 1, Academic Press, New York, 1973, p. 388, Table IV.
12. J. Y. Moisan, *Eur. Polym. J.,* **16,** 997 (1980).
13. J. P. Luongo, *Appl. Spectrosc.,* **19,** 117 (1965).
14. R. V. Albarino, *Appl. Spectrosc.,* **27,** 46 (1973).
15. J. A. J. Jacquez and H. F. Kuppenheim, *J. Opt. Soc. Am.,* **45,** 460 (1955).
16. M. W. Finkel, *Opt. Commun.,* **2,** 25 (1970).
17. C. N. R. Rao, *Ultra-Violet and Visible Spectroscopy,* Butterworths, London, 1975, p. 63, Fig. 5.2.
18. *NT Build 216, Building Materials—Polyethylene Films, Properties, and Durability,* Nordtest Method, 1982.
19. F. Gugumus, in *Plastic Additives,* 2nd ed., R. Gächter and H. Müller, Eds., Hauser, München, 1987, p. 97.

Received November 21, 1995
Accepted March 12, 1996